Polarized emission from strongly magnetized sources

Roberto Taverna*, Sergio Fabiani, Denis González Caniulef, Roberto Mignani, Fabio Muleri, Paolo Soffitta, Roberto Turolla and Silvia Zane

** Department of Mathematics and Physics, University of Roma Tre, Rome, Italy 00146*
E-mail: taverna@fis.uniroma3.it
www.matfis.uniroma3.it

Anomalous X-ray pulsars (AXPs) and soft-gamma repeaters (SGRs) form together a single class of astrophysical sources characterized by the emission of strong X-ray bursts and persistent emission with luminosity 10^{31}–10^{36} erg/s in the 0.2–10 keV energy range. These objects are commonly associated to magnetars, i.e. neutron stars endowed with ultra-strong magnetic fields. New-generation X-ray polarimeters like IXPE (NASA SMEX program), to be launched in 2021, will play a key role in assessing the nature of these sources by directly probing the star magnetic field. In fact, in the highly magnetized environment radiation is expected to be strongly polarized and such a measure will be easily within reach of IXPE. Polarization measurements will eventually confirm the presence of ultra-strong magnetic fields, probing the magnetar scenario. In this work I will discuss theoretical expectations, within the magnetar scenario, for the polarization signature of AXPs and SGRs and present numerical simulations for the response of the new-generation polarimeters currently under construction. I will also show how these sources can be used to test vacuum birefringence, a QED effect predicted by Heisemberg and Euler in the '30s and not experimentally verified as yet.

Keywords: Polarization – instrumentation: polarimeters – X-rays: stars – stars: magnetars.

1. Introduction

Soft gamma repeaters (SGRs) and anomalous X-ray pulsars (AXPs) are commonly considered to be different manifestations of the same class of isolated neutron stars (NSs), called magnetars.[1] They show a number of common distinctive properties, such as long (2–12 s) spin periods and large (10^{-13}–10^{-10} s/s) spin-down rates, which lead to magnetic dipole fields up to 10^{14}–10^{15} G, and persistent X-ray luminosities (10^{31}–10^{36} erg/s in the 0.2–10 keV range) that exceed the rotational energy loss rate (see e.g. Ref. 2 for a review). Persistent spectra are usually fitted by the superposition of a thermal (blackbody) component (with temperature ≈ 0.5 keV) at lower energies and a power-law like tail (with photon index ≈ 2–4) at higher ones. However, purely thermal spectra, characterized by the superposition of two BBs with similar temperatures, have been observed in the case of transient sources,[3] which undergo quite long (~ 1 yr) outburst phases in which the persistent flux can be enhanced up to a factor of 1000 with respect to quiescence.

The most peculiar observational manifestation of AXPs and SGRs is the emission of short (0.1–1 s), energetic (10^{38}–10^{41} erg/s) X-ray bursts and longer (1–100 s), even more energetic (10^{41}–10^{43} erg/s) flares. In the case of three SGRs, giant flares,

characterized by peak luminosities up to $\approx 10^{47}$ erg/s and long-lasting (100–1000 s) pulsating tails, modulated at the spin frequency of the star, have been detected. This phenomenology has been successfully explained in terms of the twisted magnetosphere model,[4] which invokes the occurrence of resonant Compton scattering (RCS) onto electrons flowing along the NS twisted magnetic field lines. Moreover, according to this model short bursts and intermediate/giant flares can originate either in plastic displacements of the crust (deformed under the action of the internal field toroidal component) or in sudden reconnections of the field lines high in the magnetosphere.[5,6]

In the presence of magnetar-like magnetic fields, radiation emitted from the NS surface and propagating in vacuo is expected to be linearly polarized at a high degree.[7,8] The polarization state of propagating photons (which can change due to interactions with magnetospheric particles) depends on the dielectric and magnetic properties of the vacuum around the star. These are affected by vacuum birefringence, a quantum electro-dynamics (QED) effect predicted by Heisenberg & Euler in the 1930's[9] and never tested yet, which becomes important for magnetic fields in excess of the quantum critical field $B_{\rm Q} \simeq 4.414 \times 10^{13}$ G. New polarimetric techniques developed in the last years promise to open a new window in astrophysical observations of compact objects like magnetars,[10] improving the contributions of previous X-ray polarimetry missions[11] which failed in achieving conclusive results. In this work we discuss in particular the observational prospects of the NASA SMEX mission IXPE,[12] scheduled for launch in 2021, which will allow to test vacuum birefringence and probe the existence of ultra-strong magnetic fields around magnetars.

In section 2 we illustrate the theoretical model. The issue of the polarization properties of magnetar emission is addressed in section 3. Finally, we discuss the results of some numerical simulations performed until now for IXPE in section 4 and present our conclusions in section 5.

2. Theoretical model

According to the twisted magnetosphere model,[4] the strong (up to $\approx 10^{16}$ G) internal magnetic field of magnetars is expected to be highly wound-up, with a toroidal component of the same order of magnitude of the poloidal one. This can exert a magnetic stress on the conductive surface, that can deform the crust displacing small portions of the star surface, at which the external magnetic field lines are anchored. As a result, the external field acquires in turn a toroidal component, becoming twisted. Although the twist is reasonably localized into bundles of field lines, for the sake of simplicity we will consider in the following the case of a global twist, which is characterized by the twist angle

$$\Delta\phi_{\rm N-S} = \lim_{\theta\to 0} \int_{\theta}^{\pi} \frac{B_{\phi}}{\sin\theta B_{\theta}} {\rm d}\theta \,, \tag{1}$$

where $\boldsymbol{B} = (B_{\rm r}, B_\theta, B_\phi)$ is the star magnetic field expressed in polar components (θ is the magnetic colatitude). Magnetar bursts and flares could also originate in the crustal displacements induced by the strong internal magnetic field. In fact, according to the model discussed in Ref. 5 these deformations would inject in the magnetosphere an Alfvén pulse, which dissipates into an electron-positron pair plasma, magnetically confined within the closed field line region (the so-called "trapped fireball"). The presence of this fireball can also explain the pulsating tails observed in the spectra of many burst-emitter sources (see e.g. Ref. 6 and references therein).

Since a twisted magnetic field is non-potential (i.e. $\boldsymbol{\nabla} \times \boldsymbol{B} \neq 0$), currents must flow along the closed magnetic field lines, contrary to the case of ordinary NSs, where potential (dipolar) fields are believed to be more likely. For simplicity, we assumed that the charge carriers are electrons and ions lifted from the star surface (uni-directional flow, see Refs. 4, 13, 14). These particles make the medium in which photons propagate optically thick for RCS: a scattering occurs once the resonance condition is met, i.e. when the photon energy equals the particle cyclotron energy in the particle rest frame. In particular, for a surface magnetic field strength $\approx 10^{14}$ G one finds that photons scatter onto electrons typically at a distance $r_{\rm res} \approx 10\, R_{\rm NS}$. Numerical simulations[15] show that RCS onto magnetospheric electrons can indeed account for the power-law tails observed in the soft X-ray spectra of many objects.[2,16] Resonant scatterings onto ions may also occur; however, ions are much heavier than electrons and they are lifted at much smaller heights above the star surface. At variance with electrons, one can expect that scattering onto ions can rather give origin to narrow absorption features in the spectra.[15]

3. Polarization of radiation in strong magnetic fields

Photons emitted from the surface of an ultra-magnetized NS and propagating in vacuo turn out to be linearly polarized in two normal modes, the ordinary (O) and the extraordinary (X) ones, in which the photon electric field oscillates either parallel or perpendicular to the $\boldsymbol{k}$-$\boldsymbol{B}$ plane, respectively,[7,8] where $\boldsymbol{k}$ is the photon propagation direction. The evolution of the polarization state of photons during propagation is determined by the wave equation, which can be written as

$$\boldsymbol{\nabla} \times (\bar{\boldsymbol{\mu}} \cdot \boldsymbol{\nabla} \times \boldsymbol{E}) = \frac{\omega^2}{c^2} \boldsymbol{\epsilon} \cdot \boldsymbol{E}\,, \tag{2}$$

with $\boldsymbol{E}$ the photon electric field, ω their frequency, $\boldsymbol{\epsilon}$ the dielectric tensor of the medium in which photons propagate, $\bar{\boldsymbol{\mu}}$ the inverse of the magnetic permeability tensor and c the speed of light. In general, $\boldsymbol{\epsilon}$ is expected to deviate from unity due to terms which account for plasma effects (e.g. collisions, radiation damping, etc., see Ref. 8). Photons can also change their polarization state upon scatterings with particles which flow along the closed magnetic field lines.[13–15] However, in the presence of strong magnetic fields further additional terms appear in both $\boldsymbol{\epsilon}$ and $\bar{\boldsymbol{\mu}}$, due to the vacuum polarization effect.[9] In fact, virtual electron-positron pairs, that are present in the vacuum around the star, are polarized by the strong NS field,

modifying the dielectric and magnetic properties of the vacuum. It can be shown that, close to the surface of magnetars, vacuum contributions in the dielectric tensor are by far dominant with respect to those of plasma (see e.g. Ref. 13 and references therein). Hence, neglecting the plasma terms in $\boldsymbol{\epsilon}$ one can reduce equation (2) to a simpler differential equation system,

$$\begin{aligned} \frac{\mathrm{d}Q}{\mathrm{d}z} &= -\frac{k_0\delta}{2}(2PV) \\ \frac{\mathrm{d}U}{\mathrm{d}z} &= -\frac{k_0\delta}{2}(N-M)V \\ \frac{\mathrm{d}V}{\mathrm{d}z} &= \frac{k_0\delta}{2}\left[2PQ+(N-M)U\right], \end{aligned} \tag{3}$$

where $k_0 = \omega/c$, $\delta = \alpha_{\mathrm{F}}\,(B/B_{\mathrm{Q}})^2/(45\pi)$ (with α_{F} the fine-structure constant), Q, U and V are the photon Stokes parameters and M, N and P are coefficients that depend on the star magnetic field and the $\boldsymbol{\epsilon}$ and $\bar{\boldsymbol{\mu}}$ components (see e.g. Ref. 14).

Equations (3) show that, due to vacuum polarization effects, the photon electric field evolves along a typical scale-length $\ell_{\mathrm{A}} = 2/(k_0\delta)$, which depends on B^{-2} and, through it, on the distance r from the star. So, it should be compared with the scale-length $\ell_B = B/|\boldsymbol{k}\cdot\boldsymbol{\nabla}B|$ along which the star magnetic field itself changes along the photon trajectory. This comparison allows to divide the photon propagation region into three zones:[13,17] close to the star surface, in the *adiabatic region*, $\ell_{\mathrm{A}} \ll \ell_{\mathrm{B}}$, so that the photon electric field can instantaneously adapt to the star magnetic field (which is in turn evolving along the photon trajectory), leaving unchanged the original polarization state; outward, in the *intermediate region*, $\ell_{\mathrm{A}} \simeq \ell_{\mathrm{B}}$ and the photon electric field cannot adapt so promptly as before to the star magnetic field, causing a deviation of the polarization states with respect to the emission ones; finally, in the *external region* (far from the star surface) $\ell_{\mathrm{A}} \gg \ell_{\mathrm{B}}$ and the photon electric field is practically frozen with respect to the star magnetic field, so that the polarization states can change (also dramatically) with respect to those at the emission. In fact, if the magnetic field topology in the external region is still rather chaotic the observed polarization degree turns out to be strongly reduced (even for 100% intrinsic polarization degree), due to the Stokes parameter rotation.[17]

This scenario can be further simplified by introducing the adiabatic radius,[17] or polarization limiting radius,[13] i.e. the distance at which $\ell_{\mathrm{A}} = \ell_{\mathrm{B}}$,

$$r_{\mathrm{a}} \simeq 4.8\, B_{\mathrm{p},11}^{2/5} E_1^{1/5} R_{10}^{1/5} R_{\mathrm{NS}}\,, \tag{4}$$

where $B_{\mathrm{p},11}$ is the polar magnetic field strength in units of 10^{11} G, E_1 is the photon energy in units of 1 keV and R_{10} is the NS radius in units of 10 km. Looking at equation (4) it can be seen that the adiabatic radius is larger for NSs with a stronger magnetic field and for photons with higher energy. Since the farther from the NS surface the more uniform the magnetic field topology, one can expect to observe more polarized X-ray photons for stronger magnetized NSs, with r_{a} placed at a sufficiently large distance from the star surface to prevent the original polarization pattern to be washed out by geometrical effects (see e.g. Ref. 17).

4. Numerical simulations

To implement our numerical simulations, we used the Monte Carlo code developed by Nobili, Turolla & Zane,[15] with the addition of a specific module to account for the polarization transport described in section 3. We used a globally twisted magnetic field, with the polar strength $B_{\rm p}$, the twist angle $\Delta\phi_{\rm N-S}$ and the corresponding velocity β of the magnetospheric particles as input parameters. Since for the ultra-strong magnetic fields expected in the case of magnetars the free-free opacity for X-mode photons turns out to be much suppressed with respect to that of the O-mode ones, we assumed that the emitted photons are 100% polarized in the X-mode at the surface.[13] Furthermore, owing to the fact that, in the case of interest, the adiabatic radius largely exceeds the typical radius $r_{\rm res}$ at which RCS onto magnetospheric electrons may occur, we treated separately the change in polarization state of photons due to scatterings and the evolution of the Stokes parameters determined by vacuum effects. The outputs of the Monte Carlo code are eventually reprocessed in an IDL script to account for the viewing geometry, i.e. the angles χ and ξ that the NS rotation axis makes with the observer line-of-sight (LOS) and the star magnetic axis, respectively.

We computed the observed flux, polarization degree and polarization angle (as functions of the photon energy and the rotational phase) in the case of the AXP 1 RXS J170849.0-400910 ($B_{\rm p} = 4.7 \times 10^{14}$ G, $\Delta\phi_{\rm N-S} = 0.5$, $\beta = 0.34$,

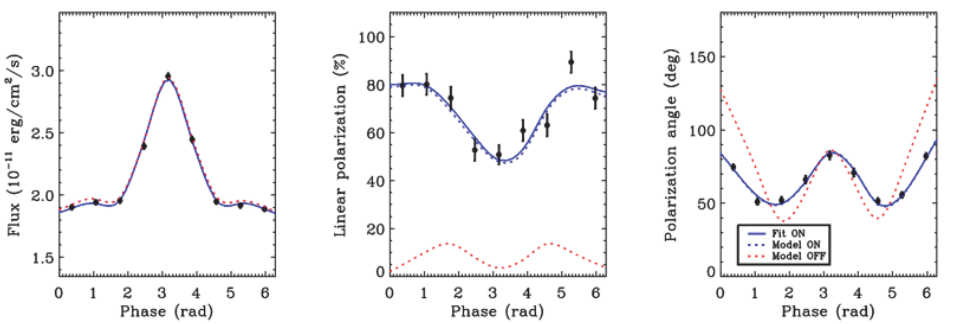

Fig. 1. Flux (left), linear polarization fraction (center) and polarization angle (right) simulated for a 250 ks observation with IXPE of the AXP 1 RXS J170849.0-400910, for $\chi = 90°$, $\xi = 60°$ and in the 2–6 keV range (filled circles with error bars). The model from which data are extracted (blue-dashed line) and that obtained for the same values of the input parameters but without accounting for QED effects (red-dashed line) are also shown. The best fit of data obtained using the entire model archive is marked by a blue, solid line.

Table 1. Input and best fit parameters of the simulation shown in Figure 1.

	χ (deg)	ξ (deg)	$\Delta\phi_{\rm N-S}$ (rad)	β	$\chi^2_{\rm red}$
Input	90	60	0.5	0.34	–
Best fit	90.36 ± 2.16	59.12 ± 1.21	0.49 ± 0.02	0.37 ± 0.07	1.25

see Refs. 18, 19), and simulated the response of the IXPE polarimeter for this source (for $\chi = 90^\circ$ and $\xi = 60^\circ$) exploiting the instrumental effective area and modulation factor. The results are shown in Figure 1: the simulated data in the 2–6 keV energy range (filled circles with error bars) are plotted as functions of the rotational phase together with the model from which they are extracted (blue-dashed line) and the same model but with QED effects turned off (red-dashed line).[14,17] A best fit of the simulated data has been then performed, using an archive of models obtained leaving the input parameters χ, ξ, $\Delta\phi_{N-S}$ and β free to vary over a wide range of values. The fit (blue-solid line in Fig. 1) recovers the original input parameters within an acceptable degree of accuracy (within 1σ, see Table 1), showing the strength of X-ray polarization measurements in extracting the physical and geometrical information of the source. Moreover, the QED-off case turns out to be ruled out at a high confidence level; this would allow us to say to have tested vacuum birefringence effects for the source at hand.

5. Discussion and conclusions

In this work we illustrated the commonly accepted theoretical model to explain the phenomenology of AXPs and SGRs, isolated NSs endowed with ultra-strong magnetic fields (magnetars). We focused in particular on the polarization of the X-ray photons emitted from these sources. In fact, radiation from magnetars is expected to be highly polarized and, due to their strong magnetic fields, these NSs are believed to be the best targets to test vacuum polarization effects, which has not been detected at the magnetic field strengths currently achievable in laboratory.

After having presented the twisted magnetosphere model and discussed the polarization evolution for photons propagating in the magnetized vacuum, we showed the output of our code in the case of the AXP 1 RXS J170849.0-400910, simulating the response of the NASA SMEX polarimeter IXPE, scheduled for the launch in 2021. Throughout our investigation, we assumed, for the sake of simplicity, that photons are emitted from the star surface 100% polarized in the X-mode. However, we point out that our code can also account for different intrinsic polarization patterns. A detailed analysis based on different, more realistic surface emission models is currently under development.

Our plots (see Fig. 1) show that X-ray polarization measurements are potentially able to distinguish between the expectations of our model with and without accounting for vacuum polarization effects. Besides to extract important information on the physics and geometry of the source (such as the values of the viewing angles χ and ξ and the parameters $\Delta\phi_{\rm N-S}$ and β, see Table 1), X-ray polarimetry will allow to test QED effects in strong magnetic fields for the first time. Furthermore, since vacuum birefringence can prevent the geometrical depolarization of the collected radiation more effectively for stronger magnetized NSs, (see Sec. 3), the detection of a high degree of polarization can be considered as an indirect evidence for ultra-strong magnetic fields in magnetars.

References

1. R. C. Duncan and C. Thompson, Formation of very strongly magnetized neutron stars - Implications for gamma-ray bursts, *ApJL* **392**, p. L9 (1992).
2. R. Turolla,S. Zane and A. L. Watts, Magnetars: the physics behind observations. A review, *Rep. Prog. Phys.* **78**, p. 116901 (2015).
3. N. Rea and P. Esposito, Magnetar outbursts: an observational review, *ASS Proc.* **21**, p. 247 (2011).
4. C. Thompson, M. Lyutikov and S. R. Kulkarni, Electrodynamics of Magnetars: implications for the persistent X-ray emission and spin-down of the soft gamma repeaters and anomalous X-ray pulsars, *ApJ* **574**, p. 332 (2002).
5. C. Thompson and R. C. Duncan, The soft gamma repeaters as very strongly magnetized neutron stars - I. Radiative mechanism for outbursts, *MNRAS* **275**, p. 255 (1995).
6. R. Taverna and R. Turolla, On the spectrum and polarization of magnetar flare emission, *MNRAS* **469**, p. 3610 (2017).
7. Yu. N. Gnedin and G. G. Pavlov, The transfer equations for normal waves and radiation polarization in an anisotropic medium , *JETP* **38**, p. 903 (1974).
8. A. K. Harding and D. Lai, Physics of strongly magnetized neutron stars, *Rep. Prog. Phys.* **69**, p. 2631 (2006).
9. W. Heisenberg and H. Euler, Consequences of Dirac's theory of the positron, *Zeitschr. Phys.* **98**, p. 714 (1936).
10. R. Bellazzini, E. Costa, G. Matt and G. Tagliaferri, X-ray polarimetry: A new Window in astrophysics, *Cambridge University Press, Cambridge* (2010).
11. M. C. Weisskopf, E. H. Silver, H. L. Kestenbaum, K. S. Long and R. Novick, A precision measurement of the X-ray polarization of the Crab Nebula without pulsar contamination, *ApJ* **220**, p. L117 (1978).
12. M. C. Weisskopf et al., in UV, X-Ray, and Gamma-Ray Space Instrumentation for Astronomy XVIII, *Proc. SPIE* **8859** (2013).
13. R. Fernández and S. W. Davis, The X-ray polarization signature of quiescent magnetars: effect of magnetospheric scattering and vacuum polarization, *ApJ* **730**, p. 131 (2011).
14. R. Taverna, F. Muleri, R. Turolla, P. Soffitta, S. Fabiani and L. Nobili, Probing magnetar magnetosphere through X-ray polarization measurements, *MNRAS* **438**, p. 1686 (2014).
15. L. Nobili, R. Turolla and S. Zane, X-ray spectra from magnetar candidates - I. Monte Carlo simulations in the non-relativistic regime, *MNRAS* **386**, p. 1527 (2008).
16. S. Mereghetti, The strongest cosmic magnets: soft gamma-ray repeaters and anomalous X-ray pulsars, *A&ARev* **15**, p. 225 (2008).
17. R. Taverna, R. Turolla, D. Gonzalez Caniulef, S. Zane, F. Muleri and P. Soffitta, Polarization of neutron star surface emission: a systematic analysis, *MNRAS* **454**, p. 3254 (2015).
18. S. A. Olausen and V. M. Kaspi, The McGill Magnetar Catalog, *ApJs* **212**, p. 6 (2014).
19. S. Zane, N. Rea, R. Turolla and L. Nobili, X-ray spectra from magnetar candidates - III. Fitting SGR/AXP soft X-ray emission with non-relativistic Monte Carlo models, *MNRAS* **398**, p. 1403 (2009).